Studies of n-Channel Organic Field-Effect Transistors Based on Naphthalene Diimide-Based Copolymers

Yen-Hsiang Wang

A thesis

submitted in partial fulfillment of the

requirements for the degree of

Master of Science

University of Washington

2023

Committee:

Samson Jenekhe

Guozhong Cao

Program Authorized to Offer Degree:

Materials Science and Engineering

University of Washington

Abstract

Studies of n-Channel Organic Field-Effect Transistors based on Naphthalene Diimide-Based Copolymers

Yen-Hsiang Wang

Chair of the Supervisory Committee:

Samson Jenekhe

Department of Chemical Engineering

I report n-channel organic field-effect transistors fabricated by PNDITz, PNDITS and a series of NDI-based random copolymers, TS_xBS, where x = 0, 10, 20, 50, consisting of naphthalene diimide (NDI), triselenophene (TS), and biselenophene (BS) to demonstrate their electrical properties. The PNDITz OFETs demonstrated poor electron mobility and high threshold voltage, whereas the PNDITS OFETs showed enhanced electron mobility ($>10^{-2}$ cm^2/Vs) with ambipolar transport properties. To

hinder the hole transport properties, we tuned the composition of donor moieties in the TS_xBS random copolymers, resulting in enhanced n-channel properties as a higher BS ratio was adopted. As the composition of the BS moiety increased to 50%, the material was demonstrated as a pure n-type semiconducting polymer. The OFET exhibited an increasing trend of on/off ratio and decreasing trend of threshold voltage with the higher BS ratio. The performance of the OFET electron mobility based on TS_xBS showed a nonlinear trend relative to the BS ratio, and the performance was optimized with TS10BS exhibiting the highest electron mobility of $1.11x10^{-1}cm^2/Vs$. Our works describe the strategy to design effective n-type polymers in terms of electrical properties suitable for efficient OFETs.

Table of Contents

List of Figures

List of Tables

List of Abbreviations

AFM	atomic force microscopy
BGBC	bottom-gate bottom-contact
BGTC	bottom-gate top-contact
BS	biselenophene
CN	chloronaphthalene
EDG	electron donating group
EWG	electron withdrawing group
FET	field-effect transistor
GIWAXS	grazing-Incidence Wide-Angle X-ray Scattering
HOMO	highest occupied molecular orbital
IPA	isopropyl alcohol
LUMO	lowest unoccupied molecular orbital
MOSFET	metal-oxide-semiconductor field-effect transistor
NDI	naphthalene diimide
ODTS	octadecyltrichlorosilane
OFET	organic field-effect transistor
OLED	organic light-emitting diode
PNDI	poly(naphthalene diimide)
PNDITS	poly(naphthalene diimide triselenophene)
PNDITz	poly(naphthalene diimide 2,5-di(thiophene-2-yl)thiazolo[5,4-d]thiazole)
PV	photovoltage
TGBC	top-gate bottom-contact
TGTC	top-gate top-contact
TS	triselenophene
TS_xBS	poly(naphthalene diimide biselenophene/triselenophene)
Tz	2,5-di(thiophene-2-yl)thiazolo[5,4-d]thiazole
UV	ultraviolet
UV-Vis	ultraviolet-visible

Acknowledgments

This work was supported by the National Science Foundation (DMR-2003518).

My special thanks to my advisor, Professor Samson Jenekhe, who allowed me to do an outstanding project on NDI-based n-channel OFETs. It gives me the opportunity to explore the world of organic electronics. I also thank Professor Guozhong Cao for attending my committee and providing valuable comments.

I would also like to thank the group mates of Jenekhe Lab, Duyen, and Sarah, who helped me with this project. Significantly, Duyen always gave me practical suggestions to overcome challenges.

Finally, I would like to express my appreciation to my family. Thank you for always supporting my dreams!

Chapter 1. Introduction

1.1. Electrical Properties in Organic Materials

In recent decades, research on transistors based on organic semiconducting materials has emerged and expanded as promising electrical devices to be applied with unique functionalities that compensate the silicon-based devices. They possess tunable bandgap energy, high transparency, stretchability, and a simple fabrication process, which encourage the researchers to concentrate on several applications, such as organic field-effect transistors (OFETs)[1], organic photovoltaic cells[2], and organic light-emitting diodes (OLEDs)[3]. Due to the advantages of low-temperature processes and fabricating on flexible polymeric substrates[4], OFETs have caught great attention in scientific communities.

1.1.a. Electronic Structure in Organic Materials

The crucial property that provides organic molecules conduct electronic charge is the conjugated π bond, alternating single and double bonds between covalently bonded carbon atoms[5]. Figure 1-1 shows the representative π-conjugated polymers. In most organic materials, carbon atoms share electrons with neighboring atoms to form covalent bonds[6]. According to molecular orbital theory, the head-to-head overlap of SP2 hybridized orbitals forms a sigma bond, and the remaining P orbital overlaps side-to-side to create a π bond in SP2 hybridization. The valence electrons tend to have the

highest energy among molecules electrons resulting from the weak interaction with molecules. That makes π-orbitals tend to be the highest occupied molecule orbital (HOMO) to accommodate valence electrons, whereas π*-orbitals, which are destructive antibonding forming by P orbitals overlap in opposite phase, are regarded as the lowest unoccupied molecule orbital (LUMO). The monomers can be linked together in conjugated polymers, allowing electrons in the π-orbitals to move across many atomic sites along the polymer chain and contribute semiconducting properties.

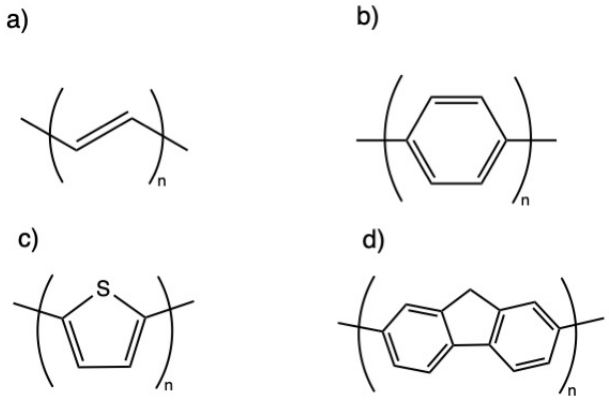

Figure 1-1 Molecular structures of some representative π-conjugated polymers.

In band theory discussed in the area of inorganic semiconductors, when the atoms are brought together to form a solid, the discrete energy levels observed in a single atom broaden by quantum mechanical effects and develop as an energy band. The energy level can be taken as continuous in the energy band. The valence electrons occupy a band of levels in the solid called the valence band. Empty states in every atom also broaden into a band of levels that is ordinarily empty, called the conduction band. The conduction band consists of π*-orbitals. Similarly, in solid-state organic

semiconducting materials, the valence band is mainly formed by π-orbitals. Van der Waals forces dominate polymers in organic solids. The weaker intermolecular interaction leads to more localized wavefunctions, which makes both the conduction band and valence band extend as tailing band, and leaves localized status in the band gap. The localized status acting as traps or recombination sites impacts the charge carrier mobility.

1.1.b. Charge Transport Properties of Semiconducting Polymers.

According to the type of the majority charge carriers, either electrons, holes, or both, polymer semiconductors can be categorized as n-type, p-type, or ambipolar polymers, respectively. Generally, an electron withdrawing group (EWG) can enhance electrophiles to attract electrons, which allows the polymers to work as n-type ones. An electron donating group (EDG) strengthens nucleophiles; the polymers exhibit p-type properties. In ambipolar polymers, both holes and electrons can be induced in the conduction channel of a single organic semiconductor layer. They can serve as complementary transistors[7] and organic light-emitting transistors.

The performance of the charge carrier transport is crucially determined by the efficiency of the charge carriers moving across intrachain or interchain. π-π stacking is a desirable stacking orientation to reduce intermolecular distance and induce stronger interchain interaction to assist carriers' transport. Charge carriers transport along

lamellar stacking orientation or backbone repeat direction tend to suffer from higher trap density due to weak interchain interaction, decreasing mobility. Crystallinity is another factor determining the charge transport properties. Polymers typically exhibit a lower degree of crystalline, and show poor performance compared to small molecule semiconductors, since the solution deposition is the primary method to process the polymer thin film layer. It is less likely to obtain a single crystal structure to facilitate charge transport properties. However, the advantage of the solution method is also apparent; it can be compatible with large-area thin film fabrication and therefore lower the manufacturing cost.

Although remarkable progress in p-type semiconducting polymers' performance has been achieved, high mobility n-type semiconducting polymers are rare due to the scarcity of materials, poor solubility, instability of charge carriers in ambient conditions, and electron trapping within the OFET. This can be done by introducing electron-withdrawing groups into the polymer structure. In recent years, semiconducting polymers with a donor–acceptor architecture have been widely studied to explore the electron transport properties. Naphthalene diimide (NDI)-based copolymers with numerous donor moieties, such as thiophene and selenophene, have been reported to achieve excellent electron mobilities (>1 cm^2/Vs)[8] and even remarkable ambipolar transport properties[9]. The large and flat backbone of the NDI moiety can minimize

disorder structure to intensify the π-π orbitals stacking. The strong electron deficient properties of the NDIs unit also reduce the electron density along the π-conjugation to achieve low-lying frontier molecular orbital energy levels. A deep LUMO energy level can be obtained to facilitate electron transport properties. Yet the electron transport properties of the NDI-based random copolymer OFETs still remain to discover[10].

1.2. OFET Devices

The most common applications for semiconducting conjugated polymers are light-emitting diodes (LEDs), solar cells, and field-effect transistors (FETs). The main advantage of conjugated polymers is the possibility of low-cost manufacturing due to the solution's processibility. This allows the use of techniques such as spin-coating, screen printing, and inkjet printing that are easily scalable to large-area substrates[11]. The large area fabrication leads to a lower cost per unit area. Another benefit is that the optoelectronic properties are tunable by molecule engineering. Conjugated polymers, therefore, could be promising candidates for the large display industry.

1.2.a. Device Geometry

The OFET consists of several electrically active layers assembled on a substrate: the organic semiconductor, the gate dielectric, and the three electrodes. The electrodes directly in contact with the active layer are named by drain and source. The electrode blocked by the insulated layer and covers the transistor channel between the source and

drain is the gate. According to the order in which the layers have been deposited, the OFET devices can be categorized as the bottom gate, bottom contacts (BGBC); bottom gate, top contacts (BGTC); top gate, bottom contacts (TGBC); and top gate, top contacts (TGTC). Among these four structures, BGBC and TGTC are the coplanar structure, which refers to the source, drain, and conducting channel placed on the same plane. The conducting channel is offset from the plane of the source and drain contacts in BGTC and TGBC, which are named as staggered structures. The structure of each device's geometry is shown in Figure 1-2.

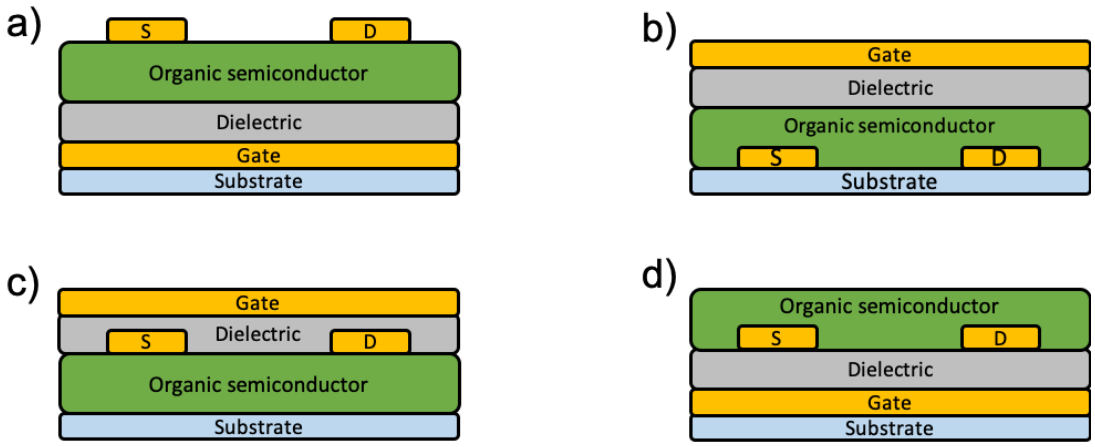

Figure 1-2 (a) bottom gate, bottom contacts (BGBC) (b) top gate, bottom contacts (TGBC) (c) top gate, top contacts (TGTC) (d) bottom gate, top contacts (BGTC)

Each of the four structures demonstrates different features and can be adapted for specific purposes. For instance, the source and drain directly contact the dielectric layer in the bottom contact structure. If inorganic material, such as SiO_2, is the dielectric layer, a high-quality contact pattern with fine feature size can be obtained by photolithography.

The semiconductor layer is deposited in the last step of the process such that the quality of the semiconductor layer can be preserved. On the contrary, it is unlikely to utilize photolithography to process the contact, followed by the deposition of the semiconductor polymer thin film in top contact structure devices. Evaporation masks are then adopted to prepare the contacts, which tend to yield poor-quality contact.

On the other hand, high carrier injection efficiency is one of the advantages of the top contact structure. As the mobility of the polymer improves, the contact resistance plays a critical factor to impede the device's performance. The charge carriers can typically be injected over a larger area in the top gate device, which is determined by the channel width and the source-to-gate overlap (L_{ov}). In bottom contact, charge carriers are injected at the edge of the source contact, which is approximately given by the contact thickness and the channel width. The contact thickness is usually in the nanoscale, whereas the gate overlap can be in the micron scale.

1.2.b. Operation and Characterization

The output and transfer curves are the two crucial characteristics of the transistors. The evolution of the drain current with increasingly gate-source voltage as the curve is measured at a giving drain-source bias, named the transfer curve, see Figure 1-3. The drain current is a function of drain-source voltage with each fixed gate-source voltage, which is known as the output curve, see Figure 1-4. The output curve and the transfer

curve can be obtained by I-V measurement. They can derive several parameters to characterize the transistors' performance, such as mobility, on/off current ratio, and threshold voltage.

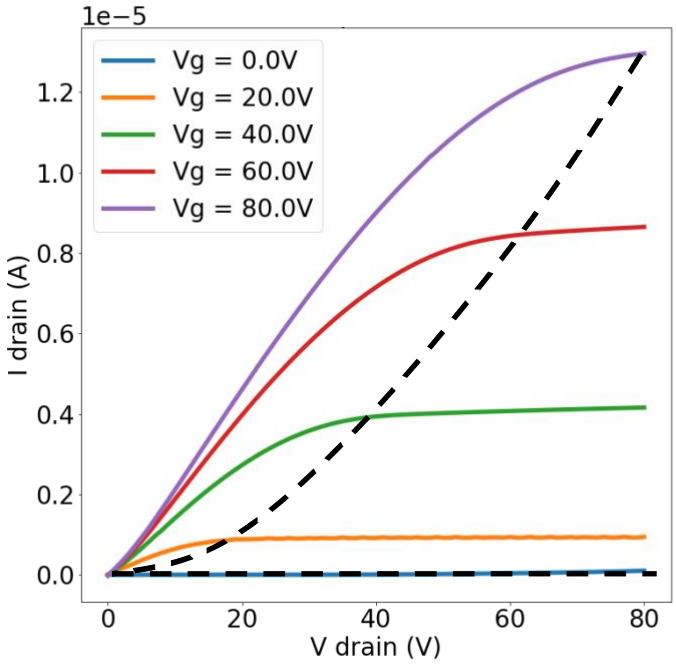

Figure 1-3 Transfer curve

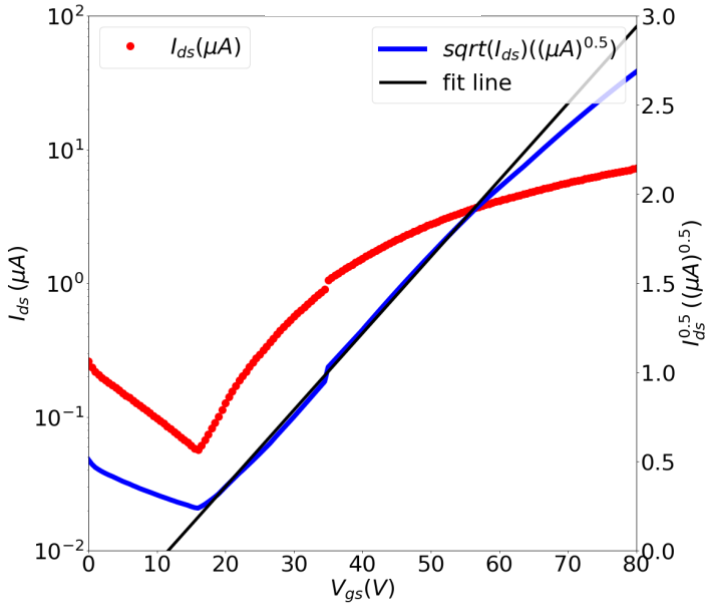

Figure 1-4 Output curve

The OFET tends to operate under accumulation mode, which refers to the current generated by the accumulation of the majority charge carriers. When no gate-source voltage is applied, no charge carrier's accumulation occurs at the semiconductor dielectric interface; the device is regarded as "off" state. Ideally, as an applied gate-source voltage polarizes the dielectric inducing the charge carriers accumulating at the surface of the semiconducting layer, the transistor turns on as "on" state. An applied drain-source voltage forces these accumulated charge carriers to transport from the source to the drain electrode, where the drain current is measured. The gate bias controls carriers flowing from source to drain under the voltage bias across the source and drain electrodes. The magnitude of the drain current is one of the critical factors in evaluating the device performance, and it depends on the majority carrier's density and mobility

in the channel. Mobility is a parameter of how fast charge carriers move in response to an external electric field.

Generally, high mobility allows the transistors to demonstrate high response speed and larger drain currents. A large drain current is desired to achieve a high speed and applicable circuit. In an actual device, the charge traps at the semiconductor-dielectric interface should be fulfilled prior to accumulating free charge carriers in the conduction channel. This trap-filling potential is called the threshold voltage (V_T) and can be determined by crystal defects, impurities, or the minority carrier density in the channel. The threshold voltage of OFET is usually higher than that of MOSFET due to the higher trap density in the amorphous structure. The on/off ratio is another essential indicator to illustrate the device performance, which is the value of "on" current (I_{on}) divided by "off" current (I_{off}). A large on/off ratio is required to distinguish both "on" and "off" states clearly.

1.3. Research Objectives

The objectives of this project are to study the unipolar and ambipolar charge transport properties of NDI-based copolymers. In this report, we demonstrated the electron transport properties of NDI-based copolymers with different donor moieties. First, we report on the electrical characterization in an OFET device configuration of the solution-processed polymer, poly(naphthalene diimide 2,5-di(thiophen-2-yl)thiazolo[5,4-d]thiazole) (PNDITz, Figure 1-5). The PNDITz OFETs were fabricated in BGBC structure and showed a mobility of the material reached 1.7 x 10^{-2} cm^2/Vs in the condition of 180°C. The threshold voltage of the devices was around 40V regardless of the annealing temperature.

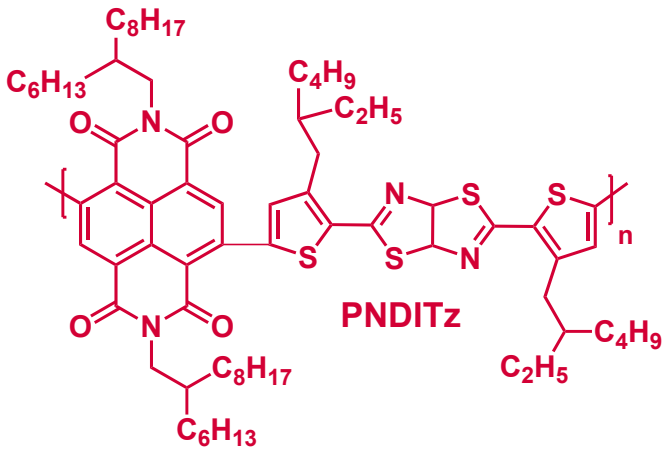

Figure 1-5 The molecular structure of PNDITz

To address the high threshold voltage issue, poly(naphthalene diimide triselenophene) (PNDITS, Figure 1-6) was applied as the active layer of the BGTC devices. The PNDITS OFETs demonstrated high electron mobility and lower threshold voltage, yet suffered from intrinsic hole carriers that generated a small amount of current in high

V_{DS} when the transistors were "off" ($V_{GS} < V_T$). To suppress the hole mobility, thinner the thickness of the active layer by increasing the spin speed and changing the work function of the electrode by using different metals (Au and Al) were taking as strategies. The improvement of suppressing the hole mobility was limited for both methods, yet the threshold voltage was significantly improved.

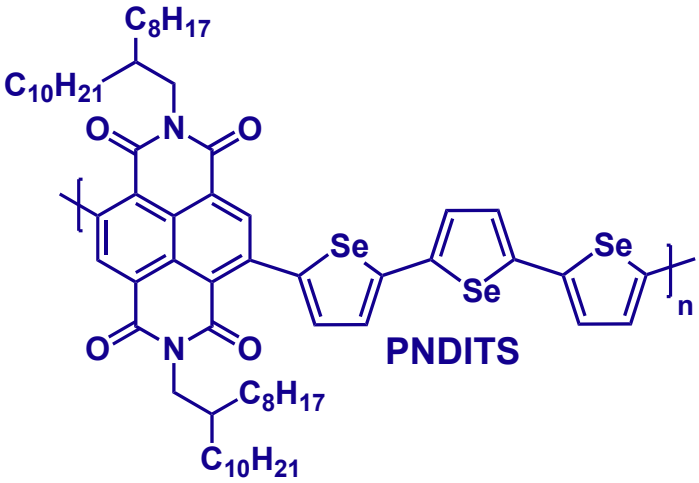

Figure 1-6 The molecular structure of PNDITS

A series of new random copolymers, poly(naphthalene diimide biselenophene/triselenophene), TS_xBS (x = 10, 20, 50, Figure 1-7), in which the biselenophene and triselenophene linkages are distributed in the chain, were applied on the OFETs as active layer to address the ambipolar transport properties of the devices. We found that the random copolymer with 50% BS composition produced OFETs with an exceed 3 x 10^{-2} cm^2/Vs electron mobility, a low threshold voltage of 10V, an improved on/off ratio of 2.4 x 10^2, and electron transport properties.

The electrical properties of OFETs based on the random copolymer donors were substantially enhanced compared to the reference PNDITS devices. The result showed that the OFETs with undesired ambipolar properties, poor on/off ratio, and threshold voltage can be improved by tuning the percentage of two different donor moieties while holding the acceptor moiety constant.

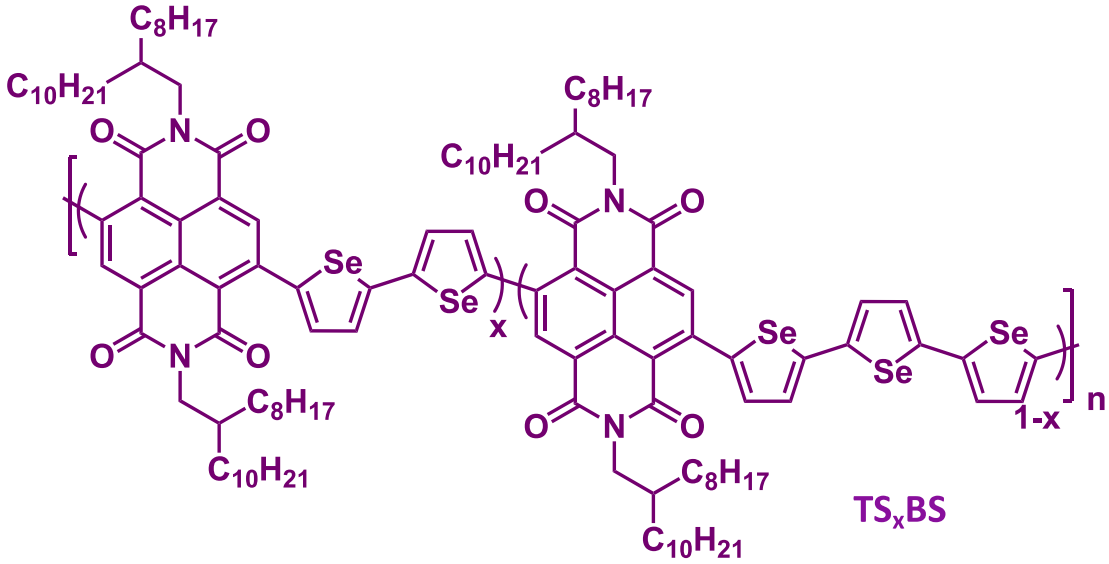

Figure 1-7 The molecular structure of TS_xBS

Chapter 2. Electron Transport Properties of Poly(naphthalene diimide 2,5-di(thiophene-2-yl)thiazolo[5,4-d]thiazole) and Poly(naphthalene diimide triselenophene)

2.1. Introduction

Achieving high mobility n-channel OFETs is one of the major challenges in the development of organic electronics. Recently, NDI-based D–A polymers with an alternating arrangement of donor and NDI units facilitated significant development in n-type OFETs, as their microstructure and electronic structure can be tailored by the appropriate choice of moieties[12]. In this chapter, the charge transport characteristics of two NDI-based polymer semiconductors, PNDITz and PNDITS, with different donor moieties were presented. The triselenophene was applied in the perspective of the larger p-orbitals of selenium, and this can enhance orbital overlap and the charge carrier mobility[13]. Field-effect electron mobility on the order of ~10^{-3} to 10^{-2} cm^2/Vs was observed from the PNDITz and PNDITS polymer semiconductors. The effects of annealing temperature on the devices' electrical performance were studied. Varying the spin speed and electrode work function as optimization strategies were applied to the PNDITS OFETs.

2.2. Experiment Methods

2.2.a. PNDITz OFET Fabrication

The PNDITz OFETs were fabricated in BGBC geometry with Si/SiO_2/Metal patterned wafers as substrates. The source/drain electrodes were patterned, defining a channel width (W) of 400 μm and length (L) of 40 μm. The substrates were ultrasonically washed with acetone, deionized water, and isopropanol (IPA) for 30 min each and then dried with nitrogen gun. The UV-plasma cleaning procedure for 10 mins was applied to remove contaminants from surfaces. The solution of ODTS with a concentration of 3mM in trichloroethylene (TCE) was spin-coated at 2000 rpm on the substrates for 30 seconds to passivate the gate oxide surface. The ODTS-treated substrates were placed together with a small vial of 30% ammonium hydroxide overnight. The ODTS-treated substrates were then sonicated with toluene for 15 min and dipped in IPA. The substrates were dried with nitrogen gun. The polymer semiconductors were spin coated onto the ODTS-treated substrate from a solution in chlorobenzene (5 mg/mL) at 2000 rpm for 60 s in a nitrogen-filled glovebox. Each film was annealed at different temperatures (180°C/200°C/220°C) for 30 min. Current–voltage characteristics of the completed devices were measured in nitrogen glove box using a Signature Probe Station. The saturation region field-effect electron mobility (μ) and threshold voltage were calculated from plots of $I_D^{1/2}$ vs. V_{GS} in a forward scan with V_{DS} at 60 V by using the equation:

$$I_{DS} = \left(\frac{W}{2L}\right)\mu C_i(V_{GS} - V_T)^2 \qquad (2-1.)$$

where I_{DS} is the drain–source current in the saturated region, W/L is the channel width to length ratio(400μm/40μm), μ is the electron field-effect mobility, C_i is the capacitance per unit area of the SiO_2 dielectric layer (11 nF/cm^2), whereas V_{GS} and V_T are the gate and threshold voltages, respectively.

2.2.b. PNDITS OFET Fabrication

Three batches of the PNDITS OFETs were fabricated in BGTC geometry. P^{2+}-Si/SiO_2 substrates were ultrasonically washed with acetone, deionized water, and isopropanol for 30 min each and then dried with nitrogen gun. The UV-ozone procedure further cleaned the substrates for 20 mins. ODTS-treated substrates were obtained by immersing the substrate in 5 mM ODTS (in toluene) at room temperature overnight. The substrates were then cleaned with toluene and IPA, dried with nitrogen, and annealed on a hotplate at the temperature of 100 °C for 10 min in nitrogen glove box.

In the first batch, the polymer semiconductors were spin coated onto the ODTS-treated substrate from a solution in chlorobenzene (6 mg/mL) at 2500 rpm for 60 s in a nitrogen-filled glovebox. Each film was annealed at various temperatures (160°C /180°C/200°C) for 20 min, and then source/drain electrodes were deposited through thermal evaporation of gold (60 nm) that defined a channel width of 1000 μm and length of 100 μm.

In the second batch, the polymer semiconductors were spin coated onto the ODTS-treated substrate from a solution in chlorobenzene (9 mg/mL). The condition of the spin-coat time was still 60 seconds, yet the spin speed for each substrate was different (2500/3000/3500/3000rpm). All the films in the batch were annealed at 200°C for 20 min, and then source/drain electrodes were deposited through thermal evaporation of gold (60 nm) that defined a channel width of 1000 μm and length of 100 μm.

In the third batch, the polymer semiconductors were spin coated onto the ODTS-treated substrate from a solution in chlorobenzene (9 mg/mL) at 3500 rpm for 60 s in a nitrogen-filled glovebox. The films were annealed at 200°C for 20 min, and then different source/drain electrodes, gold (60 nm) and aluminum (100nm), were deposited on each substrate through thermal evaporation that defined a channel width of 1000 μm and length of 100 μm.

Current–voltage characteristics of all the PNDITS devices batches were measured in nitrogen glove box using a Signature Probe Station. The saturation region field-effect electron mobility and threshold voltage were calculated from plots of $I_D^{1/2}$ vs. V_{GS} in a forward scan with V_{DS} at 80 V by using Equation (2-1).

2.3. Results and Discussion

2.3.a. Effects of Annealing Temperature on PNDITz Charge Transport Properties

The charge transport properties under different annealing temperatures of the NDI containing Tz moiety were investigated by testing OFETs with BGBC architecture. The field effect mobility in the saturation region and threshold voltage were calculated from the slope of $I_{DS}^{0.5}$ versus V_{GS} using Equation (2-1). Figure 2-1 showed the output and transfer characteristics of the PNDITz OFETs in different annealing temperatures measuring under nitrogen-filled conditions, and Table 2-1 summarizes the calculated n-channel properties, including the mobility (μ_e), the threshold voltage ($V_{T,e}$), and the on/off ratio (I_{on}/I_{off}). The average electron mobilities (μ_e^{ave}) and the average threshold voltage with error bars based on one standard deviation for each annealing temperature were shown in Figure 2-2.

The electron mobilities of the polymers decreased when the annealing temperature increased, whereas the threshold voltage didn't demonstrate a clear trend with the annealing temperature. The device annealing at 180°C gave a maximum μ_e of 1.72×10^{-2} cm^2 /Vs, yet the threshold voltage was around 40V. The PNDITz polymers showed ambipolar transport behavior from the output curves. The devices presented an I_{on}/I_{off} of 10^2 to 10^3. The result suggested that the PNDITz was not a promising n-type polymer

in the perspective of large threshold voltage, even though the electron mobility was in the order of $\sim 10^{-2}$ and $\sim 10^{-3}$ cm^2 /Vs.

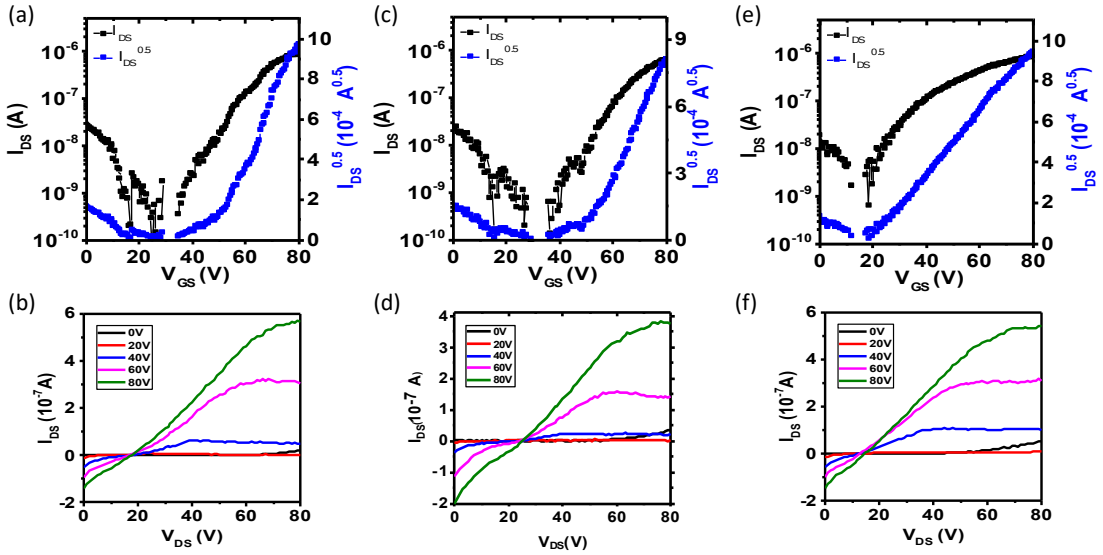

Figure 2-1 Electrical characteristics of PNDITz in the annealing temperature of (a,b) 180°C, (c,d) 200°C, (e,f) 220°C.

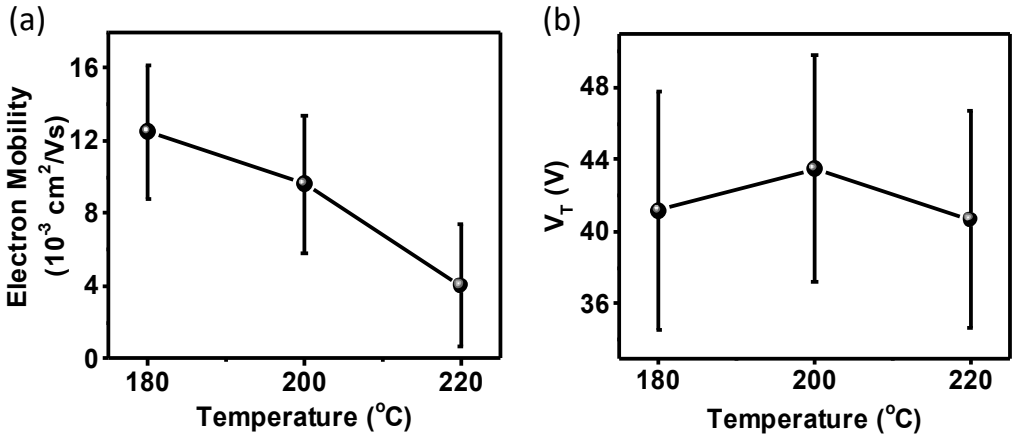

Figure 2-2 (a) Average electron mobilities and (b) average threshold voltage of PNDITz OFETs.

Table 2-1 Effect of annealing temperature on electrical properties of PNDTz OFETs with channel dimensions of 40/400 μm (L/W)

Temp. (°C)	μ_e^{ave} (μ_e^{max}) ($10^{-3}cm^2/Vs$)[a]	$V_{T,e}$ (V)[a]	I_{on}/I_{off}[a]
180	12.50±3.72 (17.2)	41.2±6.6	(8.96±6.75)x10^2
200	9.62±3.81 (13.2)	43.4±6.2	(2.90±3.17)x10^3
220	5.44±3.40 (8.18)	40.7±5.3	(1.77±0.89)x10^2

[a] Average values are obtained from at least 4 different devices.

2.3.b. Charge Carrier Transport Properties of PNDITS

2.3.b.1. Effects of Annealing Temperature on PNDITS Charge Transport Properties

To improve and investigate the charge transport properties of NDI-based polymers with different donor moieties to obtain promising n-type polymers, the triselenophene moiety was substituted as the donor unit. The charge transport properties of PNDITS polymers were calculated through the field-effect method by fabricating OFETs in BGTC architectures for different annealing temperatures. The output curves and transfer curves for the PNDITS devices for different annealing temperatures under nitrogen-filled conditions were given in Figure 2-3. The OFET parameters for both n-type and p-type characteristics, including electron and hole mobility (μ_e, and μ_e,

respectively), the ratio of electron mobility to hole mobility(μ_e/μ_h), electron and hole threshold voltage ($V_{T,\,e}$, and $V_{T,\,h}$, respectively), and on/off ratio, were presented in Table 2-2. The field effect electron mobility in the saturation region and threshold voltage were calculated from Equation (2-1). The capacitance per unit area (C_i) of the SiO_2 dielectric layer is 17 nF/ cm^2. The average field-effect electron mobility and the average electron threshold voltage with error bars based on one standard deviation for different annealing temperatures were presented in Figure 2-4.

The electron mobility and threshold voltage did not show a clear trend with annealing temperature. The on/off current ratio of the devices was low ($<10^4$) for all the annealing temperatures. As the donor moiety was substituted from Tz to TS, the average electron mobility increased five times from 1.25 x 10^{-2} cm^2/Vs to 6.28 x 10^{-2} cm^2/Vs at 180^{o}C, and the threshold voltage also decreased from 41V to 17V. All the devices showed an improvement in electron mobility and threshold voltage compared with the Tz moiety, whereas the I_{on}/I_{off} had a slightly decreased. The PNDITS showed ambipolar transport behavior. The electron mobilities and the hole mobilities were all comparable (~10^{-2} cm^2/Vs), even though the hole threshold voltage (-36V~ -47V) was much higher than the electron threshold voltage. To address the ambipolar properties and low I_{on}/I_{off}, varying the spin speed and electrode work function were applied as strategies. The results were presented in the following sections.

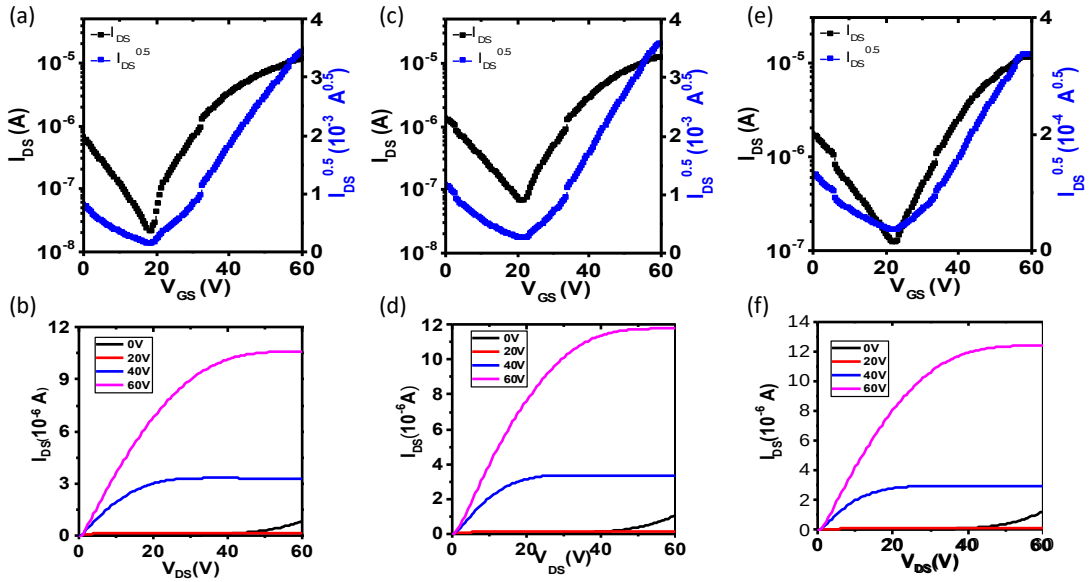

Figure 2-3 Electrical characteristics of PNDITS in an annealing temperature of (a,b) 160°C, (c,d) 180°C, (e,f) 200°C.

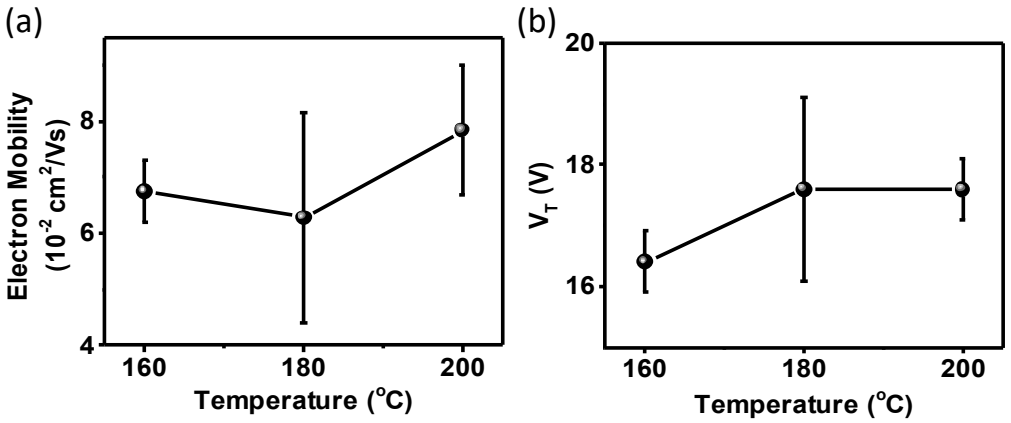

Figure 2-4 (a) Average electron mobilities and (b) average threshold voltage of PNDITS OFETs fabricated at various annealing temperatures

Table 2-2 Effect of annealing temperature on electrical properties of PNDTS OFETs

Temp. (°C)	μ_e^{ave} (μ_e^{max}) (10^{-2} cm^2/Vs)[a]	μ_h^{ave}(μ_h^{max}) ($10^{-2}$$cm^2$/Vs)[a]	μ_e/μ_h	$V_{T,e}$ (V)[a]	$V_{T,h}$ (V)[a]	I_{on}/I_{off}[a]
160	6.75±0.54 (7.14)	4.93±0.18 (5.06)	1.36	16.4±0.5	-47.7±4.7	(3.81±2.54) x 10^2
180	6.28±1.88	3.03±2.05	2.07	17.6±1.5	-36.1±4.9	(1.26±0.48) x 10^2

	(7.14)	(5.35)				
200	7.84±1.17[b] (9.24)	4.72±0.35[b] (5.16)	1.66	17.6±0.5[b]	-36.8±1.6[b]	(1.32±0.56) x 10^{2}[b]

[a] Average value is obtained from 2 different devices.

[b] Average values are obtained from at least 3 different devices.

2.3.b.2. Effects of Spin Speed on PNDITS Charge Transport Properties

To enhance the unipolar charge transport properties of PNDITS, the active layer of the OFETs were fabricated at various spin speeds, which can obtain the active layer in different thicknesses. The charge transport properties of PNDITS polymers were calculated through the field-effect method in BGTC OFET architectures. The output curves and transfer curves for the PNDITS devices for different spin speeds under nitrogen-filled conditions were given in Figure 2-5. The OFET parameters for both n-type and p-type characteristics were presented in Table 2-3. The field effect mobility in the saturation region and threshold voltage were calculated by Equation (2-1). The capacitance per unit area of the SiO_2 dielectric layer is 17 nF/cm^2. The average field-effect electron mobility and the average electron threshold voltage with error bars based on one standard deviation for different spin speeds were presented in Figure 2-6.

The electron mobility did not show a clear trend as a function of spin speed, whereas the threshold voltage significantly dropped to 15V on average as the spin speed exceeded over 3500 rpm. The ratio of the electron to hole mobility had a slightly

increasing trend from 4.18 to 10.99 as the spin speed increased, yet the PNDITS still showed ambipolar transport behavior. The I_{on}/I_{off} decreased to 10^1 as the spin speed increased to 4000 rpm. The result showed that a thinner film allows the devices to turn "on" easily, yet the issues of ambipolar transport properties and low I_{on}/I_{off} still remained to be addressed. Varying the electrode work function was applied as strategies. The results were presented in the following section.

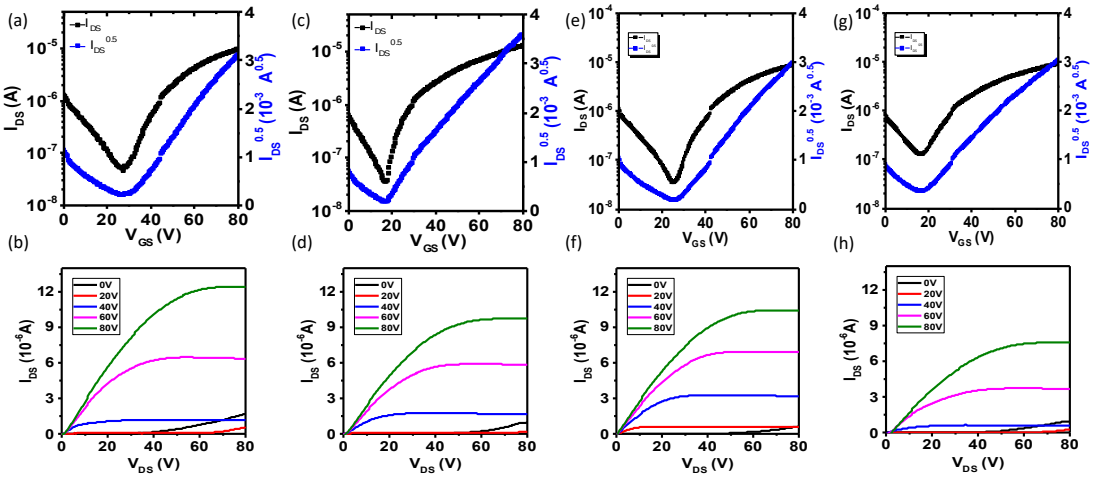

Figure 2-5 Electrical characteristics of PNDITS in a spin speed of (a,b) 2500rpm, (c,d) 3000rpm, (e,f) 3500rpm, (g,h) 4000rpm.

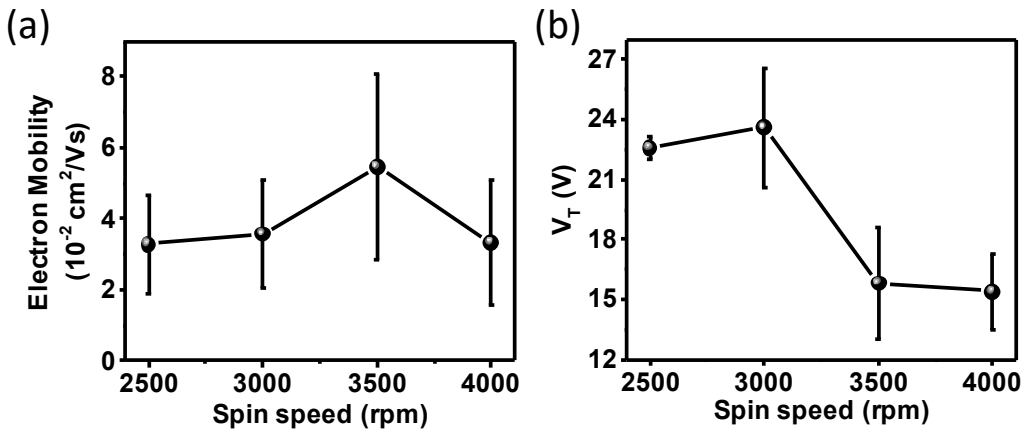

Figure 2-6 (a) Average electron mobilities and (b) average threshold voltage of PNDITS OFETs fabricated at various spin speeds.

Table 2-3 Effects of spin speed on electrical properties of PNDTS OFETs.

Spin speed (rpm)	$\mu_e^{ave}(\mu_e^{max})$ ($10^{-2}cm^2/Vs$)[a]	$\mu_h^{ave}(\mu_h^{max})$ ($10^{-3}cm^2/Vs$)[a]	μ_e/μ_h	$V_{T,e}$ (V)[a]	$V_{T,h}$ (V)[a]	I_{on}/I_{off}[a]
2500	3.29±1.38 (4.37)	7.86±5.47 (11.7)	4.18	22.6±0.6	-44±10.1	(3.59±1.03) x 10^2
3000	3.57±1.52 (5.06)	7.05±2.81 (10.1)	5.06	23.6±3.0	-48±8.1	(1.97±0.70) x 10^2
3500	5.46±2.59 (9.17)	9.08±3.19 (10.9)	6.01	15.8±2.8	-55±11.7	(2.41±1.26) x 10^2
4000	3.33±1.74 (6.27)	3.03±0.79 (3.63)	10.99	15.4±1.9	-13±3.7	(5.67±1.74) x 10^1

[a] Average values are obtained from at least 3 different devices.

2.3.b.3. Effects of Electrode Work Function on PNDITS Charge Transport Properties

In the section, the gold electrode was substituted by the aluminum electrode to investigate the effect of electrode work function (*W*) on PNDITS charge transport properties. The charge transport properties of PNDITS polymers were calculated through the field-effect method by fabricating OFETs in BGTC architectures ending with different contact electrodes (gold or aluminum). Typically, the work function of gold and aluminum is around 5.1eV and 4.1eV, respectively. The output curves and transfer curves for the PNDITS devices in different electrodes were demonstrated in

Figure 2-7. The OFET parameters for both n-type and p-type properties were calculated from at least 3 devices, and the result was given in Table 2-4. The average field-effect electron mobility and the average electron threshold voltage with error bars based on one standard deviation for different electrodes were shown in Figure 2-8. The field effect mobility and threshold voltage were calculated from Equation (2-1). The capacitance per unit area of the SiO_2 dielectric layer was 17 nF/cm^2.

As the work function decreased, the electron mobility had a slightly decreasing trend, whereas the hole mobility increased. Both electron and hole mobility were in the same order regardless of the electrode work function. Although the polymer still presented ambipolar properties, the electron threshold voltage significantly dropped to 8.4 V from 17 V in a lower work function. The hole threshold voltage also raised up to -64 V in the aluminum electrode. Even the hole threshold voltage was dramatically increased, the hole transport property had not been suppressed. The on/off ratio had a slightly improvement, yet still in the magnitude of 10^2.

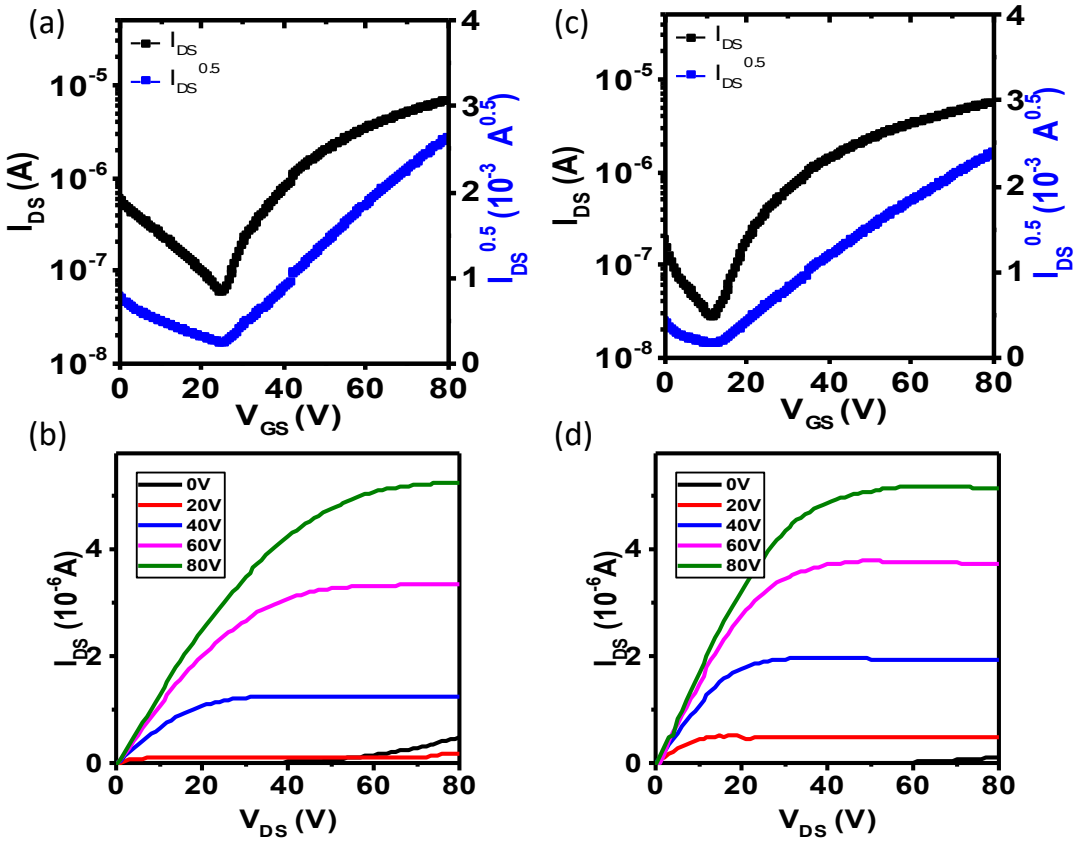

Figure 2-7 Electrical characteristics of PNDITS in an electrode work function of (a,b) 5.1eV, (c,d) 4.1eV.

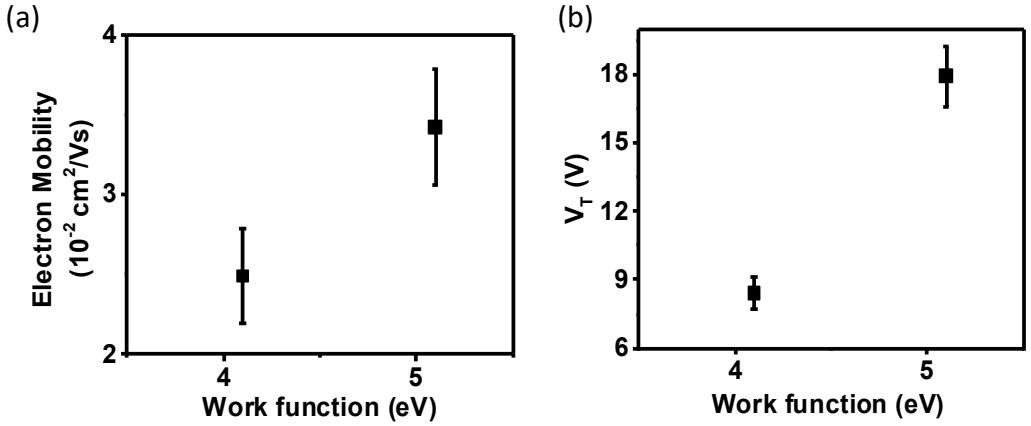

Figure 2-8 (a) Average electron mobilities and (b) average threshold voltage of PNDITS OFETs fabricated at various electrodes.

Table 2-4 Effects of electrode work function on electrical properties of PNDTS OFETs

W (eV)	$\mu_e^{ave}(\mu_e^{max})$ ($10^{-2}cm^2/Vs$)[a]	$\mu_h^{ave}(\mu_h^{max})$ ($10^{-3}cm^2/Vs$)[a]	μ_e/μ_h	$V_{T,e}$ (V)[a]	$V_{T,h}$ (V)[a]	I_{on}/I_{off}[a]
5.1	3.42±0.36 (3.97)	4.45±1.57 (7.22)	7.7	17.9±1.3	-46.9±2.2	(1.16±0.19)x10^2
4.1	2.49±0.30 (2.98)	5.51±3.58 (13.3)	4.5	8.4±0.7	-64.7±5.7	(2.05±0.79)x10^2

[a] Average values are obtained from at least 3 different devices.

2.4. Conclusions

To summarize, the charge transport properties of two NDI-based polymer semiconductors with different donor moieties, including Tz and TS, were investigated to gain insights of the properties of NDI-based n-channel OFETs. Specifically, the effects of annealing temperature on PNDITz and PNDITS OFETs were demonstrated. The optimization of the fabricating process, including varying the spin speed and the electrode work function, for evaluating the performance of PNDITS OFETs was presented. Field-effect mobility in the range of ~10^{-3}–10^{-2} cm^2/Vs with a threshold voltage of around 40V was observed from the PNDITz polymer semiconductors. The PNDITS OFETs demonstrated mobility on the order of 10^{-2} with a threshold voltage of

~ 15-22V. The I_{on}/I_{off} was around 10^2 to 10^3 for PNDITz and PNDITS OFETs. Ambipolar semiconductor performance was observed in these two polymers.

Chapter 3. Electron Transport Properties of Poly (naphthalene diimide triselenophene/biselenophene) Random Copolymers

3.1. Introduction

Developing high-performance n-channel OFETs is one of the crucial challenges in the area of organic electronics. Recently, NDI-based D–A polymers have demonstrated high charge carrier mobilities. However, due to their rather high-lying HOMO energy and low-lying LUMO energy contributed by the donor and acceptor moieties, respectively, many D–A polymers have shown ambipolar charge transport performance. Although the ambipolar polymers can be applied to the fabrication of complementary circuits, the devices suffer from high off currents and low I_{on}/I_{off} ratios[14] as the results presented in Chapter 2, which leads to high power consumption.

In this Chapter, I showed that converting ambipolar polymers into n-type polymers can be developed from new poly(naphthalene diimide triselenophene/biselenophene) random copolymers, TS_xBS (x = 10, 20, 50). The charge transport properties demonstrated a transition from ambipolar to unipolar charge transport properties with improved I_{on}/I_{off} ratio as the BS composition increased. The effects of annealing temperature on the devices' electrical performance were studied.

3.2. Experiment and Methods

The OFET devices, in BGTC architecture, were fabricated on P^{2+}-Si/SiO_2/ODTS substrates. The SiO2/Si substrates were ultrasonically washed with acetone, deionized water, and isopropanol for 30 min each and then dried with nitrogen gun. The substrates were further cleaned by the UV-ozone procedure for 20 mins. The edge of the substrates was covered by tape to keep the region from ODTS treatment. The substrates with the ODTS treatment in the center were obtained by immersing the substrates in 5 mM ODTS (in toluene) at room temperature overnight, followed by thermal annealing at 100 °C for 10 min in nitrogen glove box. The TS10BS solutions were prepared at 8 mg/mL in dichlorobenzene. The TS20BS solutions were prepared at 9 mg/mL in dichlorobenzene. The TS50BS solutions were prepared at 9 mg/mL in dichlorobenzene with 15% volume of 1-chloronaphthalene (CN) as additive. The solution was spin-coated on the substrates at 3500 rpm for 60 seconds to form active layer. Each film was then annealed at different temperatures (160°C/180°C/200°C/220°C) for 20 min before the BGTC structure was completed by 60 nm gold source/drain vapor deposition. The channel dimension of the devices was defined as a width of 1000 μm and length of 100 μm. Current–voltage characteristics of TS_xBS devices were measured in nitrogen glove box using a Signature Probe Station. The saturation region field-effect electron mobility

(μ) and threshold voltage were calculated from plots of $I_D^{1/2}$ vs. V_{GS} in a forward scan with V_{DS} at 80 V by using Equation (2-1).

3.3. Results and Discussion

3.3.a. TS_xBS Solutions

The solutions of TS_xBS random copolymer suffer from gelation at room temperature. As the amount of BS moiety increased, the gelation got severe. In the TS50BS solution, CN was added as additive to keep the solution processable. In the spin coating process, the solutions, pipette tips, and substrates are all maintained at 100°C to prevent gelation. As the portion of the BS moiety increases, the surface tension between the TS_xBS liquid and ODTS-treated surface also increases, making the liquid ball up, and leading to deposition failure. Substrates treated with ODTS in the center and surrounded by pure SiO_2 surface had been made to overcome the issue. The center ODTS-treated substrates can keep the liquid on the ODTS surface during spin coating, and therefore the liquid can spread across the ODTS-treated surface to deposit film.

3.3.b. Effects of Donor Composition on TS_xBS Charge Transport Properties

The charge transport nature of random copolymers depends upon the electron-donating ability of the donor units. Both PNDITz and PNDITS exhibited both p-type and n-type charge transport with typical ambipolar features. The charge transport properties of the NDI-based copolymers with different compositions of donor moieties fabricating under different annealing temperatures were investigated by testing OFETs

BGTC structure. The field effect mobility in the saturation region and threshold voltage were calculated by Equation (2-1). The channel width to length ratio was 1000μm/100μm, and the capacitance per unit area of the SiO_2 dielectric layer was 17 nF/cm^2. Figure 3-1 showed the output and transfer characteristics of the TS_xBS OFETs in different BS donor compositions (x= 10, 20, 50), and Table 3-1 summarizes the calculated n-channel and p-channel properties, including the electron and hole mobility, the electron and hole threshold voltage, μ_e/μ_h ratio, and on/off ratio. The average electron mobilities, hole mobility, threshold voltage, and I_{on}/I_{off} with error bars based on one standard deviation for various BS compositions in 160^{o}C annealing temperature, including x = 0, 10, 20, 50, were shown in Figure 3-2.

Although the electron mobilities of the polymers had a slight drop when BS donor composition increased, the TS_xBS polymers can still be regarded as promising n-type polymers, given that the electron mobilities were in the order of 10^{-2}. The TS10BS OFET device annealing at 160^{o}C gave a maximum μ_e of 1.11×10^{-1} cm^2 /Vs with a threshold voltage of 15 V, yet the I_{on}/I_{off} was only 10^1. As the annealing temperature increased from 160^{o}C to 220^{o}C, the electron mobility had a slight decrease from 8.47 x 10^{-2} cm^2 /Vs to 3.65 x 10^{-2} cm^2 /Vs, which can still be considered as a promising n-type material. Regardless of the annealing temperature, the TS10BS polymers still showed ambipolar transport behavior, and the hole mobilities were in the magnitude of 10^{-2},

which were comparable with the electron mobilities. The I_{on}/I_{off} of the devices dropped to 10^1 as 10 percent of TS donor was substituted by BS moiety. The result suggested that the TS10BS was not a promising n-type polymer in the perspective of low I_{on}/I_{off}, even though the electron mobility reached 10^{-1} cm^2 /Vs.

In TS20BS, although the devices were only fabricated in two different annealing temperatures (160°C and 180°C), the hole mobilities dropped significantly to 10^{-3} in both temperatures, whereas the electron mobilities slightly decreased to 3~4 x 10^{-2} cm^2 /Vs compared with the TS10BS. The devices had an enhanced electron threshold voltage of 10V at 160°C, whereas their electron threshold voltage slightly decreased to 11V at 180°C. Although the I_{on}/I_{off} in both annealing conditions were still ~10^1-10^2, it had an improvement compared with the TS10BS.

In TS_xBS polymer, including TS10BS, and TS20BS, along with the reference PNDITS, showed ambipolar characteristics and comparable electron and hole mobilities as expected from the strong electron donating group. TS50BS polymer showed unipolar charge transport properties with the highest saturation region field-effect electron mobility of 7.5 x 10^{-2} cm^2/Vs, a threshold voltage of 7V, and an on/off ratio of 10^3. The field-effect hole mobility cannot be measured and calculated in TS50BS, given that the devices did not turn “on” from the perspective of the transfer curves. The observed trend of decreasing hole mobility and threshold voltage from the

highest value in PNDITS to the lowest value in TS50BS suggested a progressive lowering of hole mobility as BS moieties were progressively substituted with TS units in the reference PNDITS. The lowest I_{on}/I_{off} (10^1) was obtained in TS10BS, and an increasing trend was observed as the BS units increased from 10 percent to 50 percent.

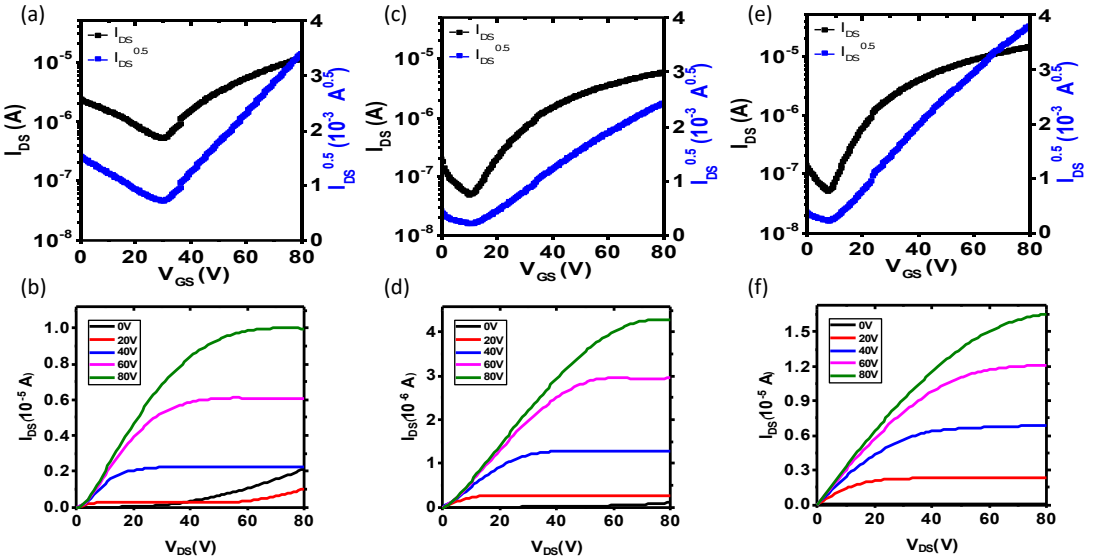

Figure 3-1 Electrical characteristics of TS_xBS in a BS composition of (a,b) 10%, (c,d) 20%, (e,f) 50%.

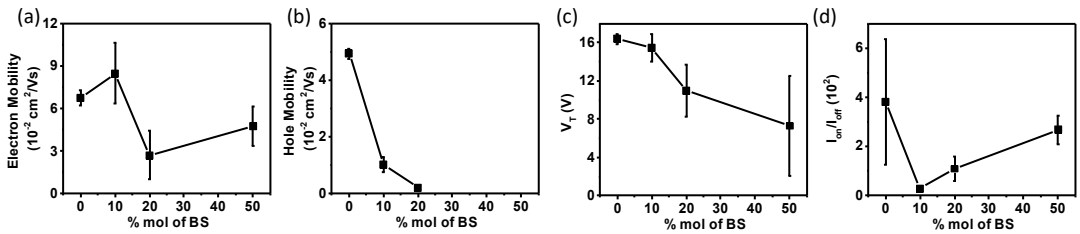

Figure 3-2 (a) Average electron mobilities, (b) average threshold voltage, (c) average threshold voltage, and (d) I_{on}/I_{off} of TS_xBS OFETs fabricated at various BS compositions.

Table 3-1 Effect of annealing temperature and BS unit composition on electrical properties of TS_xBS OFETs

x	Temp (°C)	$\mu_e^{ave}(\mu_e^{max})$[a] ($10^{-2}cm^2/Vs$)	$\mu_h^{ave}(\mu_h^{max})$[a] ($10^{-2}cm^2/Vs$)	μ_e/μ_h	$V_{T,e}$[a] (V)	$V_{T,h}$[a] (V)	On/off ratio[a]
0.1	160	8.47±2.13 (11.1)	1.03±0.21 (1.25)	8.2	15.4±1.4	-31.1±8.8	(2.99±1.07) x 10^1
	180	4.45±1.72 (7.10)	1.21±0.29 (1.60)	3.7	9.7±5.8	-40.2±4.0	(3.47±1.29) x 10^1
	200	4.82±2.68 (1.49)	1.18±0.26 (1.49)	4.1	17±3.3	-30.7±3.4	(2.87±1.12) x 10^1
	220	3.65±1.64 (1.90)	1.37±0.40 (1.90)	2.7	18±5.1	-35.5±2.5	(2.31±0.55) x 10^1
0.2	160	2.71±1.72 (3.67)	0.21±0.07 (0.27)	13.6	11.0±2.7	-51.3±2.3	(1.09±0.50) x 10^2
	180	3.35±0.35 (3.69)	0.26±0.03 (0.28)	12.9	11.4±3.6	-55.3±0.8	(9.65±2.17) x 10^1
0.5	160	4.75±1.38 (7.28)	-	-	7.3±5.2	-	(2.69±0.58) x 10^2
	180	3.82±0.58 (4.07)	-	-	13.0±1.9	-	(2.97±0.96) x 10^2
	200	5.24±1.82 (7.50)	-	-	6.1±0.9	-	(3.98±2.77) x 10^2
	220	3.09±0.51[b] (3.67)	-	-	11.3±2.7[b]	-	(2.44±0.25) x $10^{2\,b}$

[a] Average values are obtained from at least 3 different devices.

[b] Average value is obtained from 2 different devices.

3.4. Conclusions

In summary, I have investigated the charge transport properties of NDI-based random copolymer semiconductors, TS_xBS, to gain insights into the effects of donor units' composition on OFET performance. Field-effect electron mobility in the range of ~10^{-2}–10^{-1} cm^2/Vs was obtained from the polymer semiconductors. Pure n-channel OFETs were achieved by increasing the BS unit amount to 50 percent. The hole mobility and electron threshold voltage had a decreased trend, whereas the I_{on}/I_{off} had an improvement as the BS moiety increased. The results suggested that ambipolar OFETs can be transited to unipolar n-channel ones by tuning the composition of the donor units in the polymer.

Chapter 4. Conclusions and Outlook

4.1. Conclusions

In this work, I have studied factors that determine the charge transport properties of polymer semiconductors and OFETs' performance. Specifically, strategies for evaluating the electrical properties of OFETs, such as suppressing the ambipolar transport properties, decreasing the threshold voltage, increasing the electron mobilities, and I_{on}/I_{off}, were applied.

Studies of charge transport properties of NDI-based D-A copolymer semiconductors, PNDITz and PNDITS, were conducted. Compared with the PNDITz, PNDITS had enhanced electron mobilities of ~$3x10^{-2}$ -$7x10^{-2}$ cm^2/Vs, with threshold voltage ~15-23V, whereas PNDITz only had electron mobilities of ~$5x10^{-3}$- $1.2x10^{-2}$ with a relatively higher threshold voltage of ~40V. Both materials showed ambipolar charge transport properties. The electron and hole mobilities were comparable in PNDITS OFETs, and the devices suffered from low I_{on}/I_{off}.

I have fabricated TS_xBS random copolymer OFETs and found that the hole mobility can be suppressed by increasing the BS percentage to higher the hole injection barrier. Improving the threshold voltage and on/off ratio also take advantage of it. Although HOMO/LUMO energy levels have not been measured in this work, it is reasonable to infer that HOMO level will shift with the change of donor composition.

In TS_xBS random copolymer system, TS50BS OFETs annealing at 200°C have an average electron mobility of $5.24x10^{-2}cm^2/Vs$, an average threshold voltage of 6.1V, and an on/off ratio of $3.98x10^2$, which demonstrate that tuning the ratio of the donor could be as a strategy to promote the performance of NDI-based OFETs. The corresponding PNDITS devices had a $9.24\ x10^{-2}cm^2/Vs$ electron mobility with a much higher threshold voltage and lower on/off ratio. The electrical data results showed that the observed ambipolar character of TS_xBS OFETs had been modified to pure n-channel OFETs as the BS component reached 50%. The random copolymer system demonstrates a pathway for optimizing the electrical properties of the n-channel OFETs.

4.2. Outlook

In future work, thorough characterizations for the PNDITz and TS_xBS polymers remain to further understand the NDI-based polymers and n-channel OFETs. Grazing-Incidence Wide-Angle X-ray Scattering (GIWAXS) is a common tool to distinguish the stacking order of the polymer chains in thin films after deposition. The optical properties can be characterized by ultraviolet-visible (UV-Vis) light spectroscopy. The cyclic voltammetry method can investigate the precise HOMO and LUMO energy levels. The atomic force microscopy (AFM) can characterize the surface morphology of the thin film.

This random polymer strategy can also be applied in other NDI-based copolymer systems to further study and optimize the performance of n-channel OFETs. Tunning the ratio of donor components can suppress the ambipolar transport properties and can be a method to enhance the electrical properties of the devices.

Bibliography

1. Katz, H. & Bao, Z. The physical chemistry of organic field-effect transistors. *The Journal of Physical Chemistry B* **104**, 671–678 (2000).
2. Brabec, C. J., Sariciftci, N. S. & Hummelen, J. C. Plastic solar cells. *Advanced functional materials* **11**, 15–26 (2001).
3. Burroughes, J. H. *et al.* Light-emitting diodes based on conjugated polymers. *nature* **347**, 539–541 (1990).
4. Forrest, S. R. The path to ubiquitous and low-cost organic electronic appliances on plastic. *Nature* **428**, 911–918 (2004).
5. Heeger, A. J., Kivelson, S., Schrieffer, J. R. & Su, W.-P. Solitons in conducting polymers. *Rev. Mod. Phys.* **60**, 781–850 (1988).
6. Heeger, A. J. Semiconducting and metallic polymers: the fourth generation of polymeric materials. *The Journal of physical chemistry B* **105**, 8475–8491 (2001).
7. Dodabalapur, A., Laquindanum, J., Katz, H. & Bao, Z. Complementary circuits with organic transistors. *Applied Physics Letters* **69**, 4227–4229 (1996).
8. Wang, Y., Hasegawa, T., Matsumoto, H., Mori, T. & Michinobu, T. High-Performance n-Channel Organic Transistors Using High-Molecular-Weight

Electron-Deficient Copolymers and Amine-Tailed Self-Assembled Monolayers. *Advanced Materials* **30**, 1707164 (2018).

9. Guo, X., Kim, F. S., Seger, M. J., Jenekhe, S. A. & Watson, M. D. Naphthalene Diimide-Based Polymer Semiconductors: Synthesis, Structure–Property Correlations, and n-Channel and Ambipolar Field-Effect Transistors. *Chem. Mater.* **24**, 1434–1442 (2012).
10. Kolhe, N. B. *et al.* New Random Copolymer Acceptors Enable Additive-Free Processing of 10.1% Efficient All-Polymer Solar Cells with Near-Unity Internal Quantum Efficiency. *ACS Energy Lett.* **4**, 1162–1170 (2019).
11. Bao, Z. Materials and Fabrication Needs for Low-Cost Organic Transistor Circuits. *Advanced Materials* **12**, 227–230 (2000).
12. Kim, M. *et al.* Donor–Acceptor-Conjugated Polymer for High-Performance Organic Field-Effect Transistors: A Progress Report. *Advanced Functional Materials* **30**, 1904545 (2020).
13. Hwang, Y.-J., Ren, G., Murari, N. M. & Jenekhe, S. A. n-Type Naphthalene Diimide–Biselenophene Copolymer for All-Polymer Bulk Heterojunction Solar Cells. *Macromolecules* **45**, 9056–9062 (2012).
14. E. Quinn, J. T., Zhu, J., Li, X., Wang, J. & Li, Y. Recent progress in the development of n-type organic semiconductors for organic field effect transistors. *Journal of Materials Chemistry C* **5**, 8654–8681 (2017).